INSTITUTE OF PHYSICS PUBLISHING JOURNAL OF PHYSICS: CONDENSED MATTER

J. Phys.: Condens. Matter **16** (2004) S3975–S3986 PII: S0953-8984(04)78512-4

Field induced structures and phase separation in electrorheological and magnetorheological colloidal suspensions

C Métayer[1], V A Sterligov[1,2], A Meunier[1], G Bossis[1], J Persello[3] and S V Svechnikov[2]

[1] Laboratoire de Physique de la Matière Condensée, Université de Nice, Parc Valrose, 06108 Nice Cedex 2, France
[2] Institute of Semiconductor Physics, Prospekt Nauki 45, 03028 Kiev, Ukraine
[3] Université de Franche-Comté—UFR Sciences et Techniques, Laboratoire de Chimie des Matériaux et Interfaces, 16 route de Gray, 25030 Besançon, France

Received 29 March 2004
Published 10 September 2004
Online at stacks.iop.org/JPhysCM/16/S3975
doi:10.1088/0953-8984/16/38/015

Abstract

Suspensions of solid colloidal particles presenting a large mismatch of magnetic permeability or dielectric permittivity with the suspending fluid are interesting systems to correlate structure and rheology by tuning attractive dipolar forces with the help of an external field. The beginning of phase separation with formation of chainlike structure is experimentally studied in a suspension of silica particles using light scattering and in a suspension of magnetic colloidal polystyrene by means of light transmission. For a silica volume fraction of 10% we find that the mean distance between particles inside chains drops off suddenly with the increase of field. An analysis of evolution of size distribution with the field is attempted but does not show evidence for a strong increase of average sizes of chains with field. We determine the phase diagram of the magnetic suspension by measuring light transmission and show that the experimental critical volume fraction is much lower than that predicted with a theory based on transition in an isotropic medium.

(Some figures in this article are in colour only in the electronic version)

1. Introduction

Since Winslow's [1] discovery in the 1940s the field of electrorheology (ER) has emerged as a multidisciplinary field whose importance has considerably increased these last ten years. It has been the same story with magnetorheology (MR), first discovered by Rabinow [2]. The rheology of these fluids is very attractive since it can be monitored by the application of a

field—either electric or magnetic. These fluids typically consist of a suspension of highly polarizable particles in oil but we shall see that other kinds of ER and MR fluid have recently appeared. Under the application of a field there is a reversible gelation process due to the attractive interactions between the polarized particles. The most important advantages of these fluids over conventional mechanical interfaces is their ability to achieve a wide range of viscosity (several orders of magnitude) in a fraction of a millisecond. This provides an efficient way to control vibrations and many applications dealing with actuation, damping, and robotics have been patented [3]. New fields of applications are emerging such as light transmission control or elasticity control.

On the other hand, these fluids are also attractive as a model of phase separation in the presence of an anisotropic potential—the dipolar one, which can be simply controlled by the application of an external field. Such a phase separation with domain formation (usually labyrinthine structure) is well known in ferrofluids, where it is possible to successfully predict the change of period of the pattern with the amplitude of the external magnetic field, if the effective surface tension at the boundary between the two phases is known [4, 5].

More recently, well defined structures formed of cylindrical aggregates aligned on the magnetic field and arranged in a hexagonal pattern have been observed in MR suspension and this pattern can be successfully predicted [6–8]. When subjected to an oscillating shear flow these cylindrical structures transform into a striped pattern aligned in the direction of the velocity and showing a well defined period [9]. Another way to obtain a striped pattern is to apply a rotating magnetic field to the suspension because of the existence of an average attractive dipolar interaction in the plane of the rotating field [10].

The presence of a well defined pattern produced by phase separation in magnetic fluids is due to depolarization effects and does not exist in electrorheological (ER) fluids, where, at thermodynamic equilibrium, a unique domain made of a body centred tetragonal arrangement should exist. The difference of behaviour is due to the fact that the boundary conditions are different: in ER fluids, it is not the external field which is fixed but the internal field (the Maxwell field) and there is no equivalent of the demagnetization factor since the charges on the electrodes will adjust in order to keep the internal field constant. Of course, in practice, domains can also be observed in ER fluids, but they result from the kinetics of phase separation combined with the finite size of the cell. Numerous theories have been proposed to predict the formation of chains and the phase diagram [11–13], but actually the way the phase separation takes place remain unclear, in particular relative to the passage from a phase of linear chains to one of dense domains of particles. The experiments able to check these theories are very scarce due to the difficulty of characterizing well the phase of chains and the phase separation. Firstly a quite good monodisperse suspension is needed with a large enough sedimentation time—that would require small particles, but on the other hand the dipolar interaction between particles decreases as the cube of the radius of the particles, so a good compromise is usually obtained with diameters of a few hundred nanometres. Secondly the magnetic permeability or the dielectric permittivity of the particles needs to be carefully measured. Finally some relevant information on the organization of particles should be drawn from light scattering and/or neutron scattering.

This work is mainly experimental and aims to give the relevant information needed to check the theories about phase separation in colloids submitted to an external field. In section 2 we shall briefly recall the theories which are used to predict the phase separation, and then in section 3 we shall describe the experiments done to obtain the phase diagram on a magnetic colloidal suspension and compare with the theories. In section 4 we describe the results obtained with a silica suspension in the presence of an electric field with a special emphasis on the determination of interparticle distance and chain length distribution.

2. Theories of phase separation in dipolar colloids

If an isolated particle of relative magnetic permeability μ_p, surrounded by a fluid of relative permeability μ_f, is placed in an external magnetic field H_0, this particle will acquire a magnetic moment: $\mathbf{m} = 4\pi\mu_0\mu_f\beta a^3\mathbf{H}_0$; a is the radius of the particle, μ_0 the permeability of vacuum and $\beta = (\mu_p - \mu_f)/(\mu_p + 2\mu_f)$. It is worth noting that this formula also holds when the permeability of the carrier fluid is larger than that of the particle; in this case $\beta < 0$ and the magnetization vector is opposed to the field. The interaction energy between two dipoles of moment $\mathbf{m}$ is given by

$$W = \frac{1}{4\pi\mu_0\mu_f}\left(\frac{\mathbf{m}_\alpha \cdot \mathbf{m}_\beta}{r^3} - \frac{3(\mathbf{m}_\alpha \cdot \mathbf{r})(\mathbf{m}_\beta \cdot \mathbf{r})}{r^5}\right) \tag{1}$$

where $\mathbf{r}$ is the separation vector between the centres of the two particles. This energy is minimum when the two dipoles are aligned with $\mathbf{r}$ and maximum when they are perpendicular, leading to a preferential aggregation as chains of particles aligned on the direction of the field. The formation of aggregates of particles will depend on the ratio of this interaction energy to kT. Taking as reference the energy of two dipoles in repulsive configuration gives

$$\lambda = \frac{1}{4\pi\mu_0\mu_f}\frac{\mathbf{m}^2}{r^3}\frac{1}{kT} = \frac{\pi\mu_0\mu_f\beta^2 a^3 \cdot \mathbf{H}_\mathbf{0}^2}{2kT}. \tag{2}$$

For particles of diameter 1 μm with large permeability ($\beta \approx 1$) and $T = 300$ K, we obtain from (2) $\lambda = 1$ for $H = 127$ A m^{-1} (or $H = 1.6$ Oe in cgs units). This means that for usual magnetic fields the magnetic forces dominate the Brownian forces. For electric field equation (2) holds if we replace μ by ε, the dielectric permittivity.

The prediction of the average chain length as a function of λ has been derived by Cebers [11] from the calculation of the free energy of a perfect gas of chains of spheres with near neighbour dipolar interactions. Analogous results have been obtained more recently with the same kind of approach but using a derivation which can be easily extended to interacting chains [12]. The dimensionless free energy ($f = Fv/kT$) of an assembly of chains is written as

$$f = \sum_n G_n Ln(G_n/e) + 3J(\Phi)\sum_n\sum_k G_n G_k(n + k - 2/3) + U_{el}(\Phi). \tag{3}$$

The first term represents the entropy of a gas of chains with G_n the partial volume fraction of chains containing n particles. The second term is an estimate of the free energy of steric interactions between chains based on excluded volume between spherocylinders; the term $J(\Phi)$ is a function which is supposed to be independent of the size of the chains, so it is chosen in order to give the Carnahan–Starling osmotic pressure of a hard sphere:

$$J(\Phi) = (1 - 0.75\Phi)/(1 - \Phi)^2.$$

The result for g_n, the number of n-particle chains per unit volume, is

$$g_n = \frac{1}{v}e^{-nX/kT}e^{-u_n/kT} \qquad \text{and} \qquad \sum_{n=1}^{\infty} n g_n = \frac{\Phi}{v}. \tag{4}$$

The energy U_n is the energy of a chain of n particles which can include both its self-energy and the energy of interaction with an external field and other chains. These equations result from a minimization of the free energy with the constraint that the total number of particles per unit volume is given (v is the volume of a particle) and X is the Lagrange parameter. In the simplest approximation—interaction between nearest dipoles—the energy of the chain is

$u_n = -2\lambda(n-1)$ and equations (7) can be analytically solved for g_n. The result for the average number of particles per chain is [12]

$$\langle n \rangle = \frac{\sum_{n=1}^{\infty} n g_n}{\sum_{n=1}^{\infty} g_n} = y \frac{\sqrt{1+4y}-1}{1+2y-\sqrt{1+4y}} \qquad \text{with } y = \Phi e^{2\lambda}. \tag{5}$$

It is also possible, in principle, to derive a phase diagram by taking into account the existence of chains before the phase separation [13, 14]. The dimensionless free energy ($f = Fv/kT$) of an assembly of chains is written as

$$f = \sum_n G_n Ln(G_n/e) + 3J(\Phi) \sum_n \sum_k (n + k - 2/3) + \sum_n G_n u_n(\Phi). \tag{6}$$

The first term represents the entropy of a gas of chains with G_n the partial volume fraction of chains containing n particles. The second term is an estimate of the free energy of steric interactions between chains based on excluded volume between spherocylinders; the term $J(\Phi)$ is a function which is supposed to be independent of the size of the chains, so it is chosen in order to give the Carnahan–Starling osmotic pressure of a hard sphere:

$$J(\Phi) = (1 - 0.75\Phi)/(1 - \Phi)^2.$$

The last term is the electro- or magnetostatic energy, and can be obtained in the frame of mean field theory.

In the following we try to experimentally detect by means of neutron or light scattering or transmission the growth of the chains and the beginning of the phase separation in order to get a better understanding of this phase separation.

3. Field induced structure in magnetic suspensions

The suspension we have used is made of polystyrene particles (trademark Seradyn) containing inclusions (40% by weight) of magnetite. The diameter obtained by dynamic light scattering is 0.773 μm with an index of polydispersity of 2%. These particles behave as a super-paramagnetic material: they do not show any hysteresis. The magnetization curves of the suspension were measured for three different volume fractions ($\Phi = 3.5$, 10, 15%) and the initial permeability of the particles (at field lower than 30 Oe) was obtained from a fit with the Maxwell–Garnett equation.

It is worth noting that the measurement of magnetization was made at $T = -20\,^{\circ}$C in order to freeze the suspension and to prevent the particles to order during the rising of magnetic field. Otherwise use of the Maxwell–Garnett formula for isotropic repartition of particles would not be justified. The value obtained in this way was $\mu_p = 5.3 \pm 0.4$.

3.1. Phase diagram

The experiment is performed by placing the suspension between two glass slides. The thickness of the suspension is determined by that of the spacer (100 μm in our experiment) and the evaporation is prevented by sealing the cell with glue. The magnetic field is applied perpendicularly to the main plane of the cell and raised in a discontinuous way represented in figure 1(a). The interest of turning off the field for a short time ($\Delta t = 0.2$ s) is to allow the particles to move freely on a distance of about 1 radius (the Brownian time is $\tau_b = a^2/2Dt = 0.13$ s with $D = kT/6\pi\eta a$). This short period of motion in the absence of field plays an important role in preventing out-of-equilibrium aggregation and is equivalent to an annealing process. Note also that the cell is placed in a vertical position in order to minimize the effect of sedimentation. The end of phase separation can be simply observed by optical

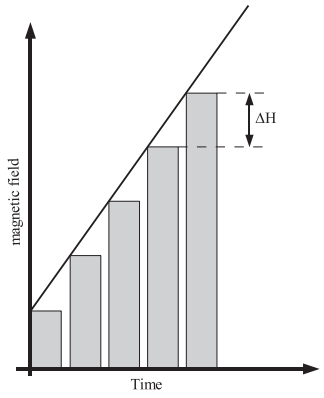

Figure 1. Ramp of magnetic field versus time. The value of increment ΔH is typically 0.04 Oe s^{-1} and the off period is 0.2 s.

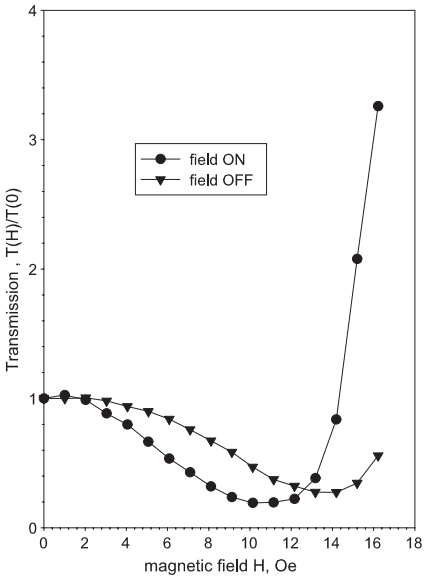

Figure 2. Light transmission versus field; the triangles represent the transmission at the end of the period with field off.

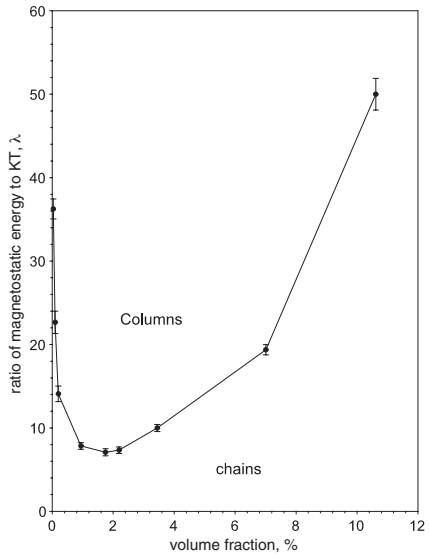

Figure 3. Experimental phase diagram obtained with colloidal magnetic polystyrene.

microscopy since the particles gather in thick aggregates which are surrounded by almost clear water, but light transmission allows us to quantify the process more efficiently and, above all, allows us to attain the very beginning of phase separation as can be seen in figure 2 which shows the light transmission versus magnetic field.

The first point is that it is possible to determine the very beginning of the structuring process at the point (here 2 Oe) where the two curves 'on' and 'off' begin to separate. Secondly and quite surprisingly, the intensity does not increase as the chain organization progresses but decreases: we shall come back to this point later on. Finally we can see that the two curves intersect at $H = 13$ Oe and after this point we have a sharp rise of the transmission curve. The rise of transmission is simply related to the formation of columnar aggregates and correlatively an increase of channels free of particles for light; the intersection point is taken as the onset of phase separation since on one hand after this point the 'on' curve is rising very quickly, due to the formation of free channels, and on the other hand the 'off' curve is lower which is coherent

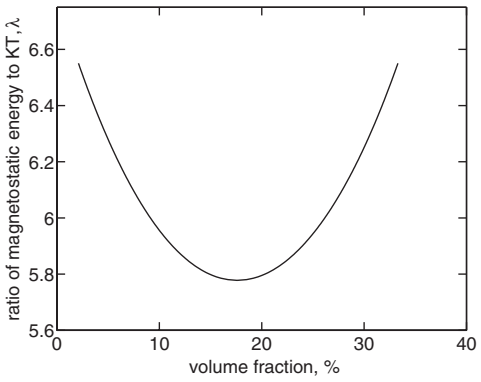

Figure 4. Theoretical phase diagram for a phase separation without chaining of particles.

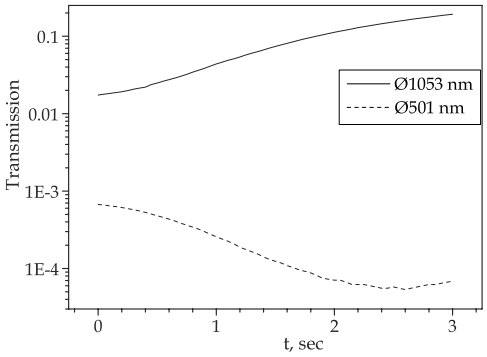

Figure 5. Light transmission of a polystyrene suspension versus time after the application of a field $E = 813$ V cm^{-1}: dashed curve, diameter 1.05 μm; solid curve, diameter 0.501 μm.

with the destruction of these free channels by the effect of diffusion of the particles outside the dense domains when the field is turned off. We have also verified that, if we stop the field around this point, the phase separation will take place after some time but the reproducibility is not very good and the uncertainty of this kind of determination of phase separation is quite large, so we shall use the intersection of the two transmission curves as criterion. We have also checked that it was independent of the rising time of the field in a quite large range (typically between 0.02 and 0.15 Oe s^{-1}; the lower limit being due to sedimentation).

The phase diagram obtained in this way is shown in figure 3. We have plotted the locus of phase separation versus the λ parameter defined in equation (2). The parameter λ is the inverse of a temperature: the phase separation occurs when λ is increased so the coexistence curve is inverted compared to the usual shape. We believe that, thanks to our procedure of turning off and on the field, coupled with light transmission, we measure the equilibrium curve; in any event the metastable range is not very important (about 10%) as we can measure from the change of transmission curve for different rates of increase of the field. The critical point occurs for a volume fraction of about 2% and with a value of λ of 7.1. The theoretical phase diagram can be obtained from equation (6).

The pressure is $P = -\left[\frac{\mathrm{d}F}{\mathrm{d}V}\right]_N$ or in dimensionless units

$$p = \frac{PV}{kT} = \Phi\frac{\partial f}{\partial \Phi} - \Phi. \tag{7}$$

Moreover, the dimensionless chemical potential $\mu\Phi/kT = f + p$.

Solving these two equations for equality of pressures and chemical potential of the two coexisting phases is difficult due to the dependence of each partial volume fraction, G_n, on average volume fraction Φ. The critical point Φ_c and λ_c is obtained by cancelling the first and second derivatives of the pressure. The curve presented in figure 4 is the solution of equation (6) in the case where the phase separation takes place directly without being preceded by the chaining process ($G_n = \Phi\delta_{n1}$). The critical volume fraction is much higher and the critical lambda much lower than the experimental ones. It is clear that a more realistic model should treat the phase separation through the growth and coalescence of chains with the help of the full solution of equation (6).

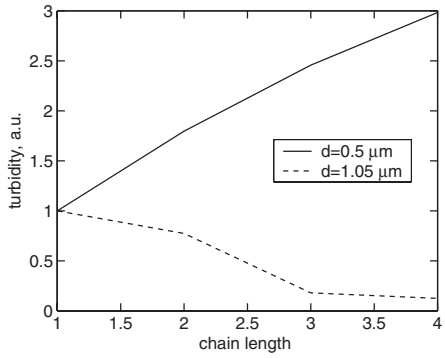

Figure 6. Theoretical transmission versus chain length obtained from 'many-particle Mie scattering'. Upper curve, diameter 1.05 μm; lower curve, diameter 0.501 μm.

3.2. Light transmission and chaining process in polystyrene suspension

Before passing to the experimental determination of chain length distribution by means of light and neutron scattering in a silica suspension we want to say a few words about the relation between light transmission and detection of chains of particles when the mismatch between refractive index is important.

Magnetic polystyrene particles are complicated scatterers since grains of magnetite inside polystyrene can absorb and scatter light inside the particles, and the strong mismatch between polystyrene ($n = 1.5905$) and water ($n = 1.33$) does not allow us to apply the Rayleigh–Gans approximation. It is possible to get some insight into the effect of multiple scattering and interferences between particles by working with bare polystyrene particles in water. The organization in a chainlike structure can be obtained in the same configuration as in figure 1 by using glass slides coated with ITO in order to apply an electric field. The frequency was set high enough to avoid the presence of ionic currents: 100 kHz. In figure 5 we have plotted transmission curves of two different monodisperse suspensions: one with a diameter of 0.501 μm and the other of 1.05 μm, after the application of an electric field $E = 813$ V cm^{-1}. We see that the transmission can increase by an order of magnitude in 3 s for the 1 μm diameter, whereas it decreases, also by an order of magnitude, with the particles of 0.5 μm.

This opposite behaviour for particles differing in diameter by a factor of two can only be interpreted in the frame of multiple scattering between particles organized in chainlike structure. The high sensitivity of light transmission to the organization of particles and to their diameter is exemplified in figure 6. The light transmission is obtained from the S matrix in the limit of zero scattering vector and the Maxwell equations are satisfied on the boundary of each sphere in the way described in [15]. In the case of isolated particles the result is that given by Mie scattering, so the transmission related to a chain of n particles is normalized by that of n isolated particles. The chains of particles are aligned with the direction of the incident beam. We actually recover qualitatively the experimental behaviour with a strong increase of transmission with the chain length for particles of diameter 1 μm and a strong decrease for particles of diameter 0.5 μm. At higher lengths the transmission can also oscillate and it would be difficult to predict an average chain length in the presence of a distribution such as that predicted by equation (1). Furthermore the measurement of the transmission as a function of the thickness of the sample shows an exponential decay which gives a characteristic length of absorption of 20 μm. It means that the light scattered by a chain is still scattered many times by others so that the resulting light transmission cannot be obtained directly from this calculation. It shows nevertheless that the decrease of transmission observed with magnetic colloidal particles is well related to the growth of chainlike structure and it can also open the way

to interesting applications in the field of active materials for the control of light transmission. If the mismatch of refractive index is low enough, then multiple scattering is low and we can use the much richer information given by the scattered light; that is the subject of the following section.

4. Determination of field induced structure by means of light scattering

Light scattering is currently used to obtain information either on the size and shape of particles or on spatial organization of particles inside colloidal suspensions. For instance the determination of size distribution of colloidal particles is realized on commercial instruments by recording the scattered light in different directions on several photodiodes (about 20) disposed both at low and large scattering angles. Using very diluted suspension the intensity scattered at different angles can be used as input of a least mean squares method based on a theoretical scattered intensity expressed as a function of the weights of the size distribution. Different numerical schemes allow us to determine the size distribution, but the refractive indices of the particles and suspending liquid need to be fairly close in order to avoid multiple scattering.

In our case we have used monodispersed silica particles with a diameter of 400 nm dispersed in 4 methylcyvlohexanol. A silane coating molecule, trimethoxysilylpropylmethacrylate, was used to ensure a good stability of the dispersion. The refractive index of the particles is close to that of the suspending fluid ($n_\mathrm{f} = 1.457$, $n_\mathrm{p} = 1.44$) so that the simple Rayleigh–Gans Debye theory can be applied without too much error. We have compared the intensity scattered by chains of different lengths using the many-particle Mie scattering calculation compared to the usual approximation given by

$$I(\mathbf{q}) \sim F(q)S(q) \quad \text{with } F(q) = (3/u^3)(\sin u - u\cos u) \quad \text{and} \quad S(\vec{q}) = N + \sum_i \sum_{j\neq i} \mathrm{e}^{\mathrm{i}\vec{q}\cdot\vec{r}_{i,j}} \tag{8}$$

where $u = qa$; $\mathbf{q} = k_\mathrm{i} - k_\mathrm{d} = 2k\sin(\theta/2)$ is the scattering vector, $F(q)$ is the form factor and $S(\mathbf{q})$ the structure factor.

The difference between the two models is small; the largest difference at high angle does not overcome a few per cent, so that we can safely use equation (8) to calculate the scattered intensity. Note that the same equation is used to interpret neutron scattering.

To our knowledge there was no attempt to determine the length distribution of elongated colloidal particles or droplets from light scattering, so we have developed our own method to get information on size distribution of elongated objects. Firstly we have used a device [16] which is able to gather all the angles scattered in one half space thanks to an elliptic mirror as shown in figure 7. The suspension is placed between a glass hemisphere HSW of diameter 10 mm and a prism P. The spacers are two copper wires of diameter 200 μm which are used as electrodes; the distance between the two parallel wires is 1.7 mm. The laser beam crosses the cell at the middle between the two electrodes and the scattering spot is placed at the first focus of the ellipsoidal mirror M. In this way, all the light scattered forward is reflected by the elliptic mirror towards its second focus where a CCD videocamera is placed. We used either a high resolution videocamera (768×512) pixels of 15 bits each, that needs a few seconds for transferring the data to the computer, or a normal videocamera for dynamic analysis. A typical image showing the effect of chaining of particles in the presence of an electric field is presented in figure 8. The white vertical line is due to the diffraction of elongated objects aligned on the horizontal axis.

The two spots on the horizontal line are the signature of the first interference order given by $\mathbf{q}\cdot\mathbf{d} = 2\pi$ where $\mathbf{d}$ is the vector joining the centres of two neighbour particles in a chain. The square in the middle of the image is the shadow of the cell (see figure 7(a)) that does not allow

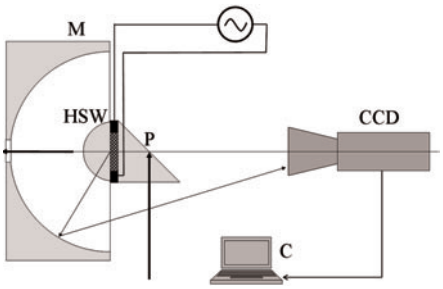

Figure 7. Schematic view of the optical device.

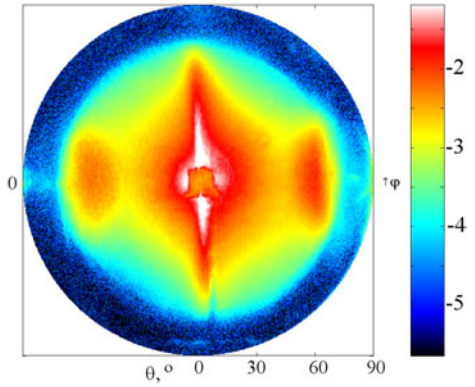

Figure 8. Scattering image (logarithmic scale) obtained on the CCD videocamera. Volume fraction $\Phi = 3\%$; field $E = 4\ \mathrm{kV\ cm^{-1}}$.

us to see the small angle structure. The small asymmetry of the image is due to slight optic misalignment. Actually, for the signal treatment we are interested only in the structure factor (see equation (8)) due to the application of the field, so we divide the image obtained with a given field by that obtained in zero field. The information we get is limited to a 2D projection of the scattering vector; so in order to obtain information on the underlying structure we have to start with a model. We can suppose a distribution of chain length defined by the partial volume fraction G_n. The average distance $\langle d \rangle$ between particles can be left as a parameter or directly taken from the measurement of the angle $2\theta_\mathrm{m}$ between the two maxima: $\langle d \rangle = \lambda/(n_\mathrm{g} \sin\theta_\mathrm{m})$ (taking into account the difference between the refractive index n_s of the suspension and that, n_g, of the glass). If we take this model of a rigid chain with a given arbitrary size distribution and calculate the scattering image, then adding 5% noise and using our numerical procedure we recover very well the initial distribution. But in practice we should consider that the chains are not perfect, so that we suppose that the distance between any pair of particles is $n\langle d \rangle + \Delta\mathbf{r}$ where $\Delta\mathbf{r}$ is a random vector described by two Gaussian distributions, one along the axis z of the chain and the other along x and y. The details of the numerical method will be described in a forthcoming paper; we only present here some typical results.

Firstly we have performed some numerical simulations with a Monte Carlo method using a Stockmayer potential (hard sphere with rigid dipole at the centre). The initial configuration was a large unique chain of 200 particles contained in a cylinder of radius $1.9a$ such that two particles cannot cross each other along the field direction. One hundred simulations of one million steps each were done with a field parameter $\lambda = 5$ and different initial configurations in order to get the coefficients G_n as well as the scattered image with good enough statistics. The scattering image ($S(\mathbf{q})$ part) is shown in figure 9 and the initial size distribution together with that calculated from the scattered image in figure 10. The result is rather good except for the smallest size whose weight in total particle number becomes too small to be found accurately.

The same numerical treatment was applied to the experimental scattering image and the result is shown in figures 11 and 12 for a field $E = 3\ \mathrm{kV\ cm^{-1}}$ and a frequency $\nu = 10\ \mathrm{kHz}$. The corresponding value of λ ($\lambda = 0.45E^2 = 4.05$ in this case) is obtained from the measurement of the dielectric permittivity, ε_s, and using $(\varepsilon_\mathrm{s} - \varepsilon_\mathrm{f})E = Nm/V$ we have m and so λ using equation (2) and assuming that m is proportional to E: $m = \alpha E$. The size distribution of chains shows a large number of isolated particles and does not contain very long chains. This is quite

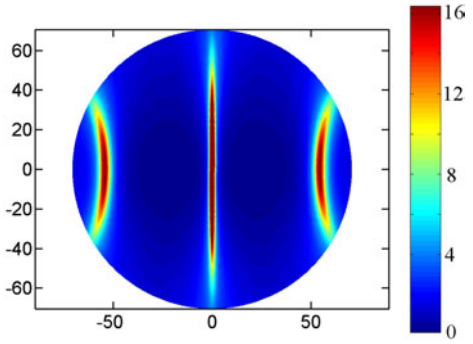

Figure 9. 'Virtual' scattering image obtained from an MC simulation at $\lambda = 5$; the image is normalized by the diffusion of isolated particles.

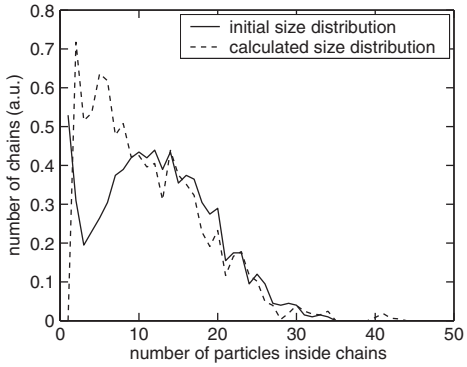

Figure 10. Comparison between size distribution calculated from MC simulation at $\lambda = 5$ and that from the treatment of the scattering image shown in figure 8.

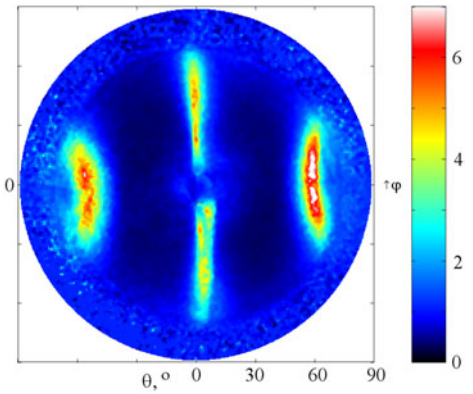

Figure 11. Experimental scattering image: $I(E)/I(E = 0)$; volume fraction $\Phi = 3\%$; $E = 3$ kV cm^{-1}.

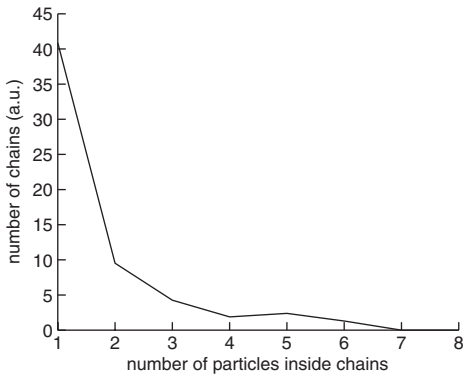

Figure 12. Size distribution obtained from experiment for $\Phi = 3\%$ and $E = 3$ kV cm^{-1}. The normalization is such that the total number of particles is 100.

obvious comparing images of figures 8 and 10 since long chains give a narrow line whereas it is rather thick in figure 10. We have calculated the size distribution obtained from equation (3) with U_n given by [14] $U_n = -4/3(\varepsilon_p - \varepsilon_f)\lambda/(\varepsilon_f + (\varepsilon_p - \varepsilon_f)\kappa(n))$ where $\kappa(n)$ is the depolarizing factor of an ellipsoid of axis ratio n and of volume nv with v the volume of a particle and n the number of particles inside the chain. The value of ε_p, the permittivity of the ellipsoid, is evaluated from the permittivity measured at $\Phi = 10\%$ by $\varepsilon_p - \varepsilon_f = (\varepsilon(\Phi) - \varepsilon_f)/\Phi$. The average size of chains predicted by this model is 87, that is to say about 40 times the experimental value.

This huge difference between theory and experiment is difficult to explain. We could envisage that the broadening should be due to multiple scattering, but the volume fraction is low and we have verified by calculation that multiple diffusion does not play a significant role inside a chain; furthermore, the analysis of neutron scattering gives a size distribution quite close to that obtained by light scattering. We shall come back to this discussion in the conclusion.

Let us now look to other information: the average distance between particles inside chains. The first order interference gives a distance between particles $\langle d \rangle = \lambda/(n_g \sin(\theta))$ with n_g the

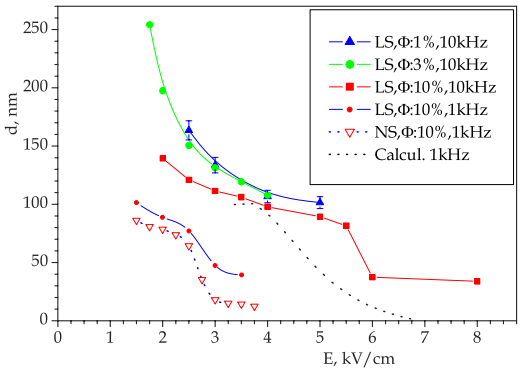

Figure 13. Distance between two spheres inside chains versus electric field for three volume fractions. The lower curve has been obtained from neutron scattering (NS).

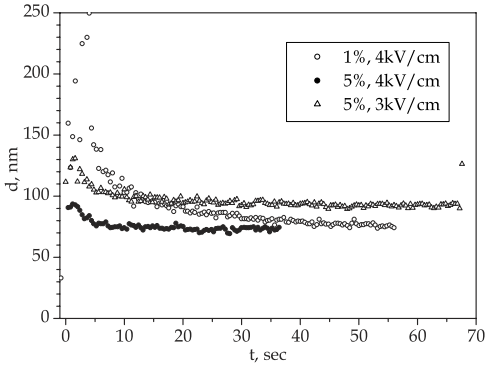

Figure 14. Dynamic of chain formation after the application of the field; d is the average distance between two neighbouring particles.

refractive index of a glass hemisphere and θ the angle corresponding to the peak intensity. It is drawn in figure 13 for three different volume fractions, $\Phi = 1\%$, 3%, and 10%, and a frequency of 10 and for 1 kHz at 10%.

As we could expect this average distance does not depend too much on the volume fraction and strongly decreases when we increase the field. The difference of distance between 1 and 10 kHz is due to the increase of permittivity when the frequency is decreased: for 1 kHz we measured $\lambda = 1.5E^2$ instead of $0.45E^2$ for 10 kHz; this behaviour is characteristic of ionic polarization due to water present inside the silica particle. The lower curve is obtained by neutron scattering and shows a reasonable agreement with light scattering. We must keep in mind that with our geometry in light scattering we cannot access a distance smaller than $\lambda/n_s = 437$ nm whereas with neutrons these are the largest distances which are difficult to attain. An interesting observation with the 10% volume fraction is a quite sharp decrease of interparticle distance with field which is found both by light and neutron scattering. The average distance can be estimated by the following Boltzmann average:

$$\langle d \rangle = \int_0^R \int_0^1 u \mathrm{e}^{-\frac{\lambda}{r^3}(3u^2-1)} r^3 \,\mathrm{d}r \,\mathrm{d}u \Big/ \int_0^R \int_0^1 \mathrm{e}^{-\frac{\lambda}{r^3}(3u^2-1)} r^2 \,\mathrm{d}r \,\mathrm{d}u.$$

The dotted curve represents the theoretical curve. If the order of magnitude is the right one the shape is quite different since there is now abrupt change followed by a levelling. It is likely that this behaviour is an indication of some non-linear change in the interaction potential between the particles which no longer follow the dipolar model. Finally, we have reported in figure 14 the dynamics of the chaining process by recording with a videocamera the change of position of the diffraction peaks. We see that, for 3 kV cm^{-1}, the time of formation is about 10 s. The time needed for two particles to approach from 150 to 50 nm can be easily

calculated in the bipolar approximation. Taking into account the slowing down due to increase of hydrodynamic resistance gives a time of about 0.5 s, that is to say one order of magnitude faster than that observed experimentally. This is another clue to the presence of existence of a short range repulsive force.

5. Conclusion

We have determined the phase diagram of a magnetic colloidal suspension using light transmission and a particular annealing process which consists in interrupting the field for a short period of time. The phase diagram shows a critical value of the control parameter $\lambda = 7$ and a critical volume fraction $\Phi_c = 2\%$. The model of phase separation from an isotropic suspension cannot explain these values which will be the basis of a further test of theories taking into account the chain formation before phase separation.

Besides, we have found by studying light transmission in polystyrene suspensions that the chaining of particles could lead either to a strong decrease or a strong increase of transmission depending on the size of the particles.

The analysis of field induced structuring of silica suspension by light and neutron scattering has shown that the distance between particles inside chains present a quite abrupt change with the field and then a levelling. This behaviour is probably the indication of the presence of another kind of interaction between particles than the pure dipolar one. We have developed an experiment and a numerical analysis capable of obtaining the size distribution of chains of particles from a light or neutron scattering experiment. From this analysis we find that the growth in the size of the chains with the field remains small compared to the theoretical predictions. This can also be related to the presence of another interparticle interaction different from the dipolar one. Due to the presence of an ionic layer it is possible that alternative field induces some electroconvection around the particles and creates an effective repulsion between particles.

Acknowledgments

We acknowledge Institute Laue Langevin for access to their neutron line and we thank P Lindner for helpful discussion.

References

[1] Winslow W M 1949 *J. Appl. Phys.* **20** 1137
[2] Rabinow J 1948 *AIEE Trans.* **67** 1308
[3] Carlson J D 2002 *Proc. 8th Int. Conf. on ER Fluids and MR Suspensions (Nice 9–13 July 2001)* ed G Bossis, World Scientific, pp 63–9
[4] Cebers A 1990 *Magnetohydrodynamics* **26** 309–13
[5] Buyewitch Yu A and Zubarev Yu A 1993 *J. Physique* II **3** 1633
[6] Lemaire E, Bossis G and Grasselli Y 1993 *J. Physique* II **2** 359
[7] Flores G A, Liu J, Mohebi M and Jamasbi N 1999 *Phys. Rev.* E **59** 751–62
[8] Grasselli Y, Bossis G and Lemaire E 1994 *J. Physique* II **4** 253
[9] Cutillas S, Bossis G and Cebers A 1998 *Phys. Rev.* E **57** 804
[10] Carletto P, Bossis G and Cebers A 2002 *Int. J. Mod. Phys.* B **16** 2279–85
[11] Cebers A O 1974 *Magn. Gidrodin.* **2** 36
[12] Zubarev A Y 2001 *Colloid J.* **61** 338
[13] Teixeira J C 1998 *Phys. Rev.* E **57** 1752
[14] Zubarev A Y and Iskakova L Y 2003 *Colloid J.* **65** 150–65
[15] Van de Hulst H C 1981 *Light Scattering by Small Particles* (New York: Dover)
[16] Sterligov V A and Cheyssac P 2001 *Patent CNRS* no 0115232